Journal of Molecular Catalysis A: Chemical 397 (2015) 127–133

Contents lists available at ScienceDirect

Journal of Molecular Catalysis A: Chemical

journal homepage: www.elsevier.com/locate/molcata

Oxidation states of active catalytic centers in ethanol steam reforming reaction on ceria based Rh promoted Co catalysts: An XPS study

Erika Varga, Zsuzsa Ferencz, Albert Oszkó, András Erdőhelyi, János Kiss*

Department of Physical Chemistry and Materials Science of the University of Szeged, Aradi vértanúk tere 1, H-6720 Szeged, Hungary

ARTICLE INFO

Article history:
Received 1 August 2014
Received in revised form
26 September 2014
Accepted 11 November 2014
Available online 15 November 2014

Keywords:
Steam reforming of ethanol
Hydrogen production
Cobalt–ceria catalyst
Rhodium promoter
XPS

ABSTRACT

X-ray photoelectron spectroscopic (XPS) investigations were carried out to study the oxidation states of CeO_2 and CeO_2 supported Co–Rh catalysts during the temperature programmed stream reforming of ethanol reaction (SRE). Gas chromatography also was used to analyze the product composition. An initial re-oxidation of the pre-reduced catalysts was observed by water reactant and our results revealed a tendency of the oxidized monometallic catalysts to promote aldol condensation-type reactions. It was found that Rh enhances the reduction of Co during the pretreatment, and the highest H_2 selectivity was obtained with the bimetallic catalyst in SRE reaction. Moreover, acetone formation was negligible on this sample. Enhanced C—C bond scission and hydrogen production were detected from 650 K. In contrast to pure ethanol decomposition, during the EtOH + H_2O reaction minor but important changes could be detected on the Ce 3d spectra. It was concluded that the accumulation of strongly bonded carbide species in the case of Co/CeO_2 catalyst can contribute to the decreasing activity. This type of carbon was absent in the presence of a trace amounts of Rh, therefore the catalyst was more stable.

1. Introduction

Sustainable development requires new alternative cheap and renewable sources of energy. Great efforts are currently made to produce hydrogen, e.g., for fuel cell applications by heterogeneously catalyzed processes. This demand inspired studies of the dehydrogenation of oxygenated hydrocarbons [1–3]. In particular, the light alcohol ethanol is an important candidate as a chemical hydrogen carrier. Noble metals, especially Rh, are proved to be excellent catalysts for the dehydrogenation reaction [4], but their prices are prohibitively high. As an alternative, the less expensive transition metal Co is considered to be a promising catalyst for the steam reforming of ethanol (SRE) [5–10]. In addition, a mixture of carbon dioxide and methane can serve as a feed for the catalytic production of hydrogen by dry reforming of methane (DRM) [11,12] where cobalt containing catalysts may have an important role. During SRE, acidic supports like Al_2O_3 favor dehydration and thereby increase the tendency for coke formation due to the polymerization of ethylene [13–15]. However, on ceria (CeO_2), which is considered to be a basic support, dehydration is limited and its redox properties hinder coke formation [5,16]. The oxygen exchange capacity of cerium oxide is associated with its ability to reversibly change the cerium oxidation states between Ce^{4+} and Ce^{3+} [17–19]. All these observations led to the outstanding attention to the catalytic properties of Co/ceria system in SRE.

Naturally, the surface properties of the metal and of the oxide support, and also the metal/oxide interface determine the formation and stability of the intermediates present in the ethanol transformation processes. It is generally accepted that the primary step in alcohol activation is the formation of alkoxide [20]. Depending on the particular metal, dehydrogenation and C—C bond scission lead to the formation of alkoxide, oxametallacycle, aldehyde, acyl and coke on the surface and mostly H_2, CH_4, CO, CO_2 and aldehyde in the gas phase [21–30]. Recent studies suggested that Co^{2+} sites are the active centers in SRE, and Co^0 sites are responsible for coke formation [29,30], while other authors considered metallic cobalt to play the key role in SRE [32]. High pressure X-ray photoelectron spectroscopic studies (HPXPS) demonstrated that at a constant ethanol (without water) pressure of 0.1 mbar the reduction of Ce^{4+} to Ce^{3+} increased significantly between 320 and 600 K due to a higher mobility of oxygen or Ce^{3+} centers at elevated temperatures. No coke formation was observed up to 600 K on CeO_2. During the reaction of ethanol with the Co/CeO_2(1 1 1) model catalyst the amount of Co^{2+} decreased drastically with increasing temperature, and at 600 K the majority of Co was metallic; this process was accompanied by a severe reduction of the ceria [33].

* Corresponding author. Tel.: +36 62 544803; fax: +36 62 544106.
E-mail address: jkiss@chem.u-szeged.hu (J. Kiss).

http://dx.doi.org/10.1016/j.molcata.2014.11.010
1381-1169/

Very recently we have found that trace amounts of rhodium promoter (0.1%) dramatically altered the reaction pathways of SRE on Co/ceria catalysts. In contrast to Co/ceria, on rhodium containing Co/ceria catalysts acetone was not observed. Addition of a small amount of Rh as promoter to the Co/CeO_2 catalyst, however, resulted in a significant increase in the hydrogen selectivity [34]. These very important findings motivated us to establish the oxidation state of the catalytically active sites before and after the catalytic reaction of ethanol + water (SRE) on pure ceria, Co/ceria and Rh + Co/ceria catalysts by X-ray photoelectron spectroscopy (XPS).

2. Experimental procedure

The catalysts preparation and characterization methods were detailed elsewhere [34]. The ceria supported Co catalysts were prepared by impregnating the support CeO_2 (Alfa Aesar, 43 m^2/g) with the aqueous solution of $Co(NO_3)_2$ to yield a nominal metal content of 2 wt% (0.056 mol%). The impregnated powders were dried at 383 K, calcined at 973 K and pressed to pellets. The Rh–Co bimetallic samples were prepared by sequential impregnation (impregnation with Co first, then the same procedure after impregnation with 0.1 wt% Rh −0.0017 mol%). After calcined at 973 K the BET surface areas of the CeO_2 support, the 2% Co/CeO_2 and of the 0.1% Rh + 2% Co/CeO_2 catalysts were 21.5 m^2/g, 7.4 m^2/g and 7.6 m^2/g, respectively, while the average pore sizes were between 14.4 and 12.3 nm, which is consistent with a mesoporous material [9,34]. Before the measurements, fragments of catalyst pellets were oxidized at 673 K in flowing O_2 for 20 min and reduced at 773 K in flowing H_2 for 60 min in the catalytic reactor.

Catalytic reactions were carried out in a fixed-bed continuous-flow reactor (200 mm long with 8 mm i.d.), which was heated externally. The dead volume of the reactor was filled with quartz beads. The operating temperature was controlled by a thermocouple placed inside the oven close to the reactor wall, to assure precise temperature measurement. For catalytic studies small fragments (about 1 mm) of slightly compressed pellets were used. Typically, the reactor filling contained 50 mg of catalyst. In the reacting gas mixture the ethanol:water molar ratio was 1:3. The ethanol–water mixture was introduced into an evaporator with the help of an HPLC pump (Younglin; flow rate: 0.007 ml liquid/min); the evaporator was flushed with Ar flow (60 ml/min). Argon was used as a carrier gas (60 ml/min). The reacting gas mixture-containing Ar flow entered the reactor through an externally heated tube in order to avoid condensation. The space velocity was 72,000 h^{-1}. The samples were heated in the gas mixture from 373 to 773 K at a rate of 3 K/min.

The analysis of the products and reactants was performed with an Agilent 6890 N gas chromatograph using HP-PLOT Q column. The gases were detected simultaneously by thermal conductivity (TC) and flame ionization (FI) detectors. To increase the sensitivity of CO and CO_2 detection a methanizer was applied before the detectors.

The amount and the reactivity of surface carbon formed in the catalytic reactions were determined by temperature-programmed hydrogenation. After performing the reactions of ethanol–water mixture at 823 K for 120 min the reactor was flushed with Ar at the reaction temperature; then the sample was cooled to 373 K, the Ar flow was changed to H_2, and the sample was heated up to 1173 K with a 10 K/min heating rate. The formed hydrocarbons were determined by gas chromatography.

For XPS studies, the powder samples were pressed into pellets with ca. 1 cm diameter and a few tenth of mm thickness. Sample treatments were carried out in a high-pressure cell (catalytic chamber) connected to the analysis chamber via a gate valve. The samples were pre-treated in the same way as described above. After the pre-treatment, they were cooled down to room temperature in flowing nitrogen. Then, the high-pressure cell was evacuated; the sample was transferred to the analysis chamber in high vacuum (i.e., without contact to air), where the XP spectra were recorded. As the next step, the sample was moved back into the catalytic chamber, where it was treated with the reacting gas mixture at the reaction temperature under the same experimental conditions as used for the catalytic reaction. XP spectra were taken with a SPECS instrument equipped with a PHOIBOS 150 MCD 9 hemispherical electron energy analyzer, using Al K_α radiation ($h\nu$ = 1486.6 eV). The X-ray gun was operated at 210 W (14 kV, 15 mA). The analyzer was operated in the FAT mode, with the pass energy set to 20 eV. The takeoff angle of electrons was 20° with respect to surface normal. Typically five scans were summed to get a single spectrum. For data acquisition and evaluation both manufacturer's (SpecsLab2) and commercial (CasaXPS, Origin) software were used. The binding energy scale was corrected by fixing the Ce 3d u‴ peak (see below) to 916.6 eV.

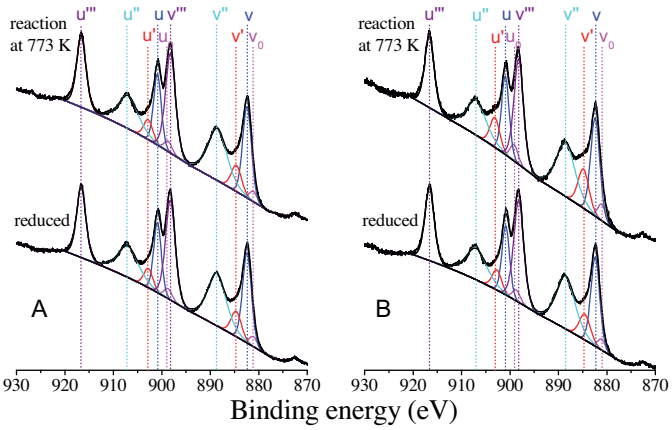

Fig. 1. Ce 3d spectra before and after SRE reaction on reduced ceria (A) and on 0.1% Rh + 2% Co/ceria catalysts.

3. Results and discussion

Based on former studies [34,35], it can be concluded that the oxidized and reduced ceria is not fully inactive either in the decomposition of ethanol or in the SRE reaction. On the CeO_2 support (without cobalt and rhodium), initially only acetaldehyde was formed (at 3–5% ethanol conversion), but between 650 and 800 K (where the ethanol conversion was ~25–30%) the main product was ethylene besides the less amount of acetone and CO_2.

The Ce 3d spectra of reduced ceria before and after SRE reaction at 773 K are shown in Fig. 1A. Generally, the Ce 3d region of CeO_2 is rather complex, i.e., it is composed of three doublets, (u‴, v‴), (u″, v″) and (u, v) corresponding to the emissions from the spin-orbit split $3d_{3/2}$ and $3d_{5/2}$ core levels of Ce^{4+}. The three doublets are assigned to different final states: u‴ (916.6 eV) and v‴ (898.4 eV) are due to a $Ce^0 3d^9 4f^0$ O $2p^6$ final state, u″ (907.7 eV) and v″ (889.0 eV) to a Ce $3d^9 4f^1$ O $2p^5$ final state, and u (900.9 eV) and v (882.5 eV) to a Ce $3d^9 4f^2$ O $2p^4$ final state [36,37]. A minor reduction of Ce^{4+} to Ce^{3+} is best detectable as the small intensity increase of the u′ (903.9 eV) and v′ (885.3 eV) peaks and also the weaker u_0 (899.3 eV) and v_0 (880.2 eV) components, which are characteristic of Ce^{3+}. Interestingly, this spectral feature of ceria did not change after the reaction with ethanol–water mixture at 773 K (Fig. 1A). To quantify the amount of Ce^{3+}, the ratio of the integrated peak areas of Ce^{3+} spectral contributions to the total Ce 3d spectrum, i.e., $Ce^{3+}/(Ce^{3+} + Ce^{4+})$ was used. The Ce^{3+} content was 11%

during the whole process. This is in contrast with the ethanol–ceria interaction without water, where the reduction of Ce^{4+} to Ce^{3+} was more pronounced between 320 and 600 K due to a higher mobility of oxygen or Ce^{3+} centers at elevated temperatures [33]. It seems that the dissociation of water in SRE could re-oxidize the Ce^{3+} centers.

On 2% Co/CeO_2 the conversion of the ethanol and the product distribution in SRE reaction are displayed in Fig. 2A. At low conversion up to 500 K, acetaldehyde and acetone were detected in the gas phase. From 500 to 700 K, the acetaldehyde selectivity attenuated, while the selectivities of H_2, ethylene and CO_2 increased moderately and the main carbon-containing product still was acetone. Above 700 K the dominant products were H_2, acetaldehyde, ethylene, CO_2, CO, and methane. The main effect of Co as compared to the pure CeO_2 case was manifested in the medium temperature range (650–750 K) as the increased conversion, accompanied by enhanced selectivities for acetone and H_2 at the expense of ethylene (Fig. 2A). The main reaction route of acetaldehyde formation is the dehydrogenation of ethoxy species [34]:

$$C_2H_5O_{(ads)} \rightarrow CH_3CHO_{(ads)} + H_{(ads)} \quad (1)$$

Acetaldehyde desorbs either as a product or immediately oxidizes to surface acetate species by lattice oxygen or by OH groups.

The other reaction path is the formation of acetone ($CH_3COCH_{3(g)}$), which is the dominant product at medium temperatures in our case. According to the literature data, acetone can be produced through aldol condensation of acetate (Reaction (2)) or via the reaction of acetyl groups (CH_3CO) with methyl species (Reactions (3)–(5)) [5,34,38]:

$$2CH_3COO_{(ads)} \rightarrow CH_3COCH_{3(g)} + CO_2 + O_{(ads)} \quad (2)$$

$$CH_3CHO_{(ads)} \rightarrow CH_3CO_{(ads)} + H_{(ads)} \quad (3)$$

$$CH_3CO_{(ads)} \rightarrow CH_{3(ads)} + CO \quad (4)$$

$$CH_3CO_{(ads)} + CH_{3(ads)} \rightarrow CH_3COCH_{3(g)} \quad (5)$$

At ~800 K, the conversion and the H_2 selectivity transiently dropped, which was also seen as an increase in the acetaldehyde selectivity. A possible reason is the acetaldehyde desorption and recombination/reduction with hydrogen forming ethanol.

$$CH_3CHO_{(a)} + 2H_{(a)} \rightarrow CH_3CH_2OH_{(g)} \quad (6)$$

In order to get closer to the clarification of surface mechanism, we identified the oxidation state of cobalt and ceria before and after reaction at different temperatures. In Fig. 4A we display some Co $2p_{3/2}$ photoemissions from the 2% Co/ceria sample. After oxidation at 673 K the signal from Co^{2+} appeared at 780.4 eV with the characteristic shake-up satellite at 786.2 eV. After reduction at 773 K, the peak positions practically did not change, but a smaller reduced state was developed (777.8 eV), it means that Co is hardly reducible at this temperature. After the reduction procedure, some intensity decrease was observed. This change may be attributed to the sintering and some encapsulation of cobalt clusters by support. After reactions at 473 and 623 K the Co was mainly in oxidized state. The deconvoluted peaks obtained after reduction and after reaction at 473 K are displayed in Fig. 6A. The satellite peak at 786.2 eV remained also detectable which also supports the presence of oxidized Co. It is worth mentioning that Co^{2+} gained intensity after the reaction at 473 and 623 K which could be explained by some disruption of Co clusters due to strong interaction with the reactants. Following the 773 K post-reaction of Co/ceria the Co $2p_{3/2}$ spectrum showed a weak shoulder at 777.8 eV due to a slight reduction of Co^{2+} (Fig. 4A and 6A). The change in its intensity after the reaction at 773 K may reflect a slight encapsulation by ceria support or covering by carbon species formed in the catalytic process (see Fig. 7). Sintering or diffusion of cobalt into the bulk also cannot be excluded. After a careful analysis of the Ce 3d spectra of Co/ceria catalyst (not shown) we may conclude that the SRE reaction (in contrast to the decomposition reaction of ethanol without water) caused only a minor additional reduction in ceria. It should be mentioned that using pure ethanol in the interaction with Co/ceria, the ceria became more and more reduced with increasing reaction temperature [33]. It is very probable that water during the SRE reaction may serve sufficient OH groups to re-oxidize the reduced center of ceria.

The acetaldehyde formation below 600 K and high acetone production between 500 and 750 K suggests a propensity of the oxide phases for aldol condensation-type reactions since our catalyst contains a significant number of Co^{2+} sites and ceria is still oxidized in this temperature range in the steam reforming (SRE) reaction. In harmony with the literature data [5] and our recent findings the acetone formation may be attributed to the unreduced, nearly stoichiometric ceria support [34].

Before turning to the Rh promoted Co/ceria system, we summarize the product distribution and the conversion of ethanol obtained on ceria supported small amount of Rh without Co (Fig. 2B). On 0.1% Rh/CeO_2 initially acetaldehyde and small amounts of CO and methane were formed, but between 650 and 800 K the main products were hydrogen, acetone, and CO_2. As the Rh surface concentration was very low the ethanol conversion was also low, at 770 K it was not more than 58–60%. The Rh XPS signals obtained before and after SRE at 473, 623 K and 773 K are displayed in Fig. 4B. After oxidation the Rh $3d_{3/2}$ appeared at 309.2 eV, while the Rh $3d_{1/2}$ was detected at 314.0 eV. After reduction at 773 K, the Rh $3d_{3/2}$ moved to 307.4 eV. This value is somewhat higher (by 0.3 eV) as was observed on bulk phase metallic rhodium. This binding energy difference can be attributed to the small particle size of Rh clusters on ceria. The peak position did not alter after the reaction (Fig. 4B).

The presence of a small amount of Rh in Co/ceria catalyst increased the ethanol conversion and basically altered the product distribution of SRE reaction, significantly increased the hydrogen selectivity (Fig. 2C). The most catalytic and spectroscopic measurements were carried out on 0.1% Rh + 2% Co/CeO_2 catalyst. The Co/Rh atomic ration is 33.0 in this case. On the Rh-promoted Co/CeO_2 catalyst, below 550 K the products were acetaldehyde, methane and CO. Between 600 and 750 K hydrogen, methane, CO, CO_2, and acetaldehyde were detected, and around 800 K (where the ethanol conversion reaches 90–95%), hydrogen and CO_2 were dominant, but CH_4 and CO as well as small amounts of ethylene and acetaldehyde were also formed (Fig. 2C). It is worth emphasizing that acetone was not detected at any temperature on the Rh-promoted Co/CeO_2 catalyst, in spite of the fact that around 700 K it was the major hydrocarbon product adsorbed on 2% Co/CeO_2 and on 0.1% Rh/CeO_2, and it was well detectable even on CeO_2 at the same temperature.

To obtain additional information, time-dependent isothermal measurements were carried out at 723 K. Fig. 3A and B display the ethanol conversion and hydrogen selectivity as a function of reaction time on different ceria based catalysts. It is clearly seen that the most efficient was the Rh promoted Co/ceria catalyst. In order to point out the efficiency of the 0.1% Rh promoter, we performed some experiments with a Rh-free 10% Co/CeO_2 catalyst. Fig. 3A and B clearly demonstrates that the effect of 0.1% Rh on 2% Co/CeO_2 is more significant than the increase in Co loading in terms of both conversion and selectivity.

One of the most important XPS observations is that rhodium promoted the reduction of cobalt at 773 K. Fig. 5A and 6B show that in the reduction process the Co $3d_{3/2}$ is split up, a new component belonging to metallic Co developed as a shoulder at 777.8 eV. The effect can be explained by the hydrogen spillover phenomenon [34,39]. The promoting effect of noble metals on the reduction

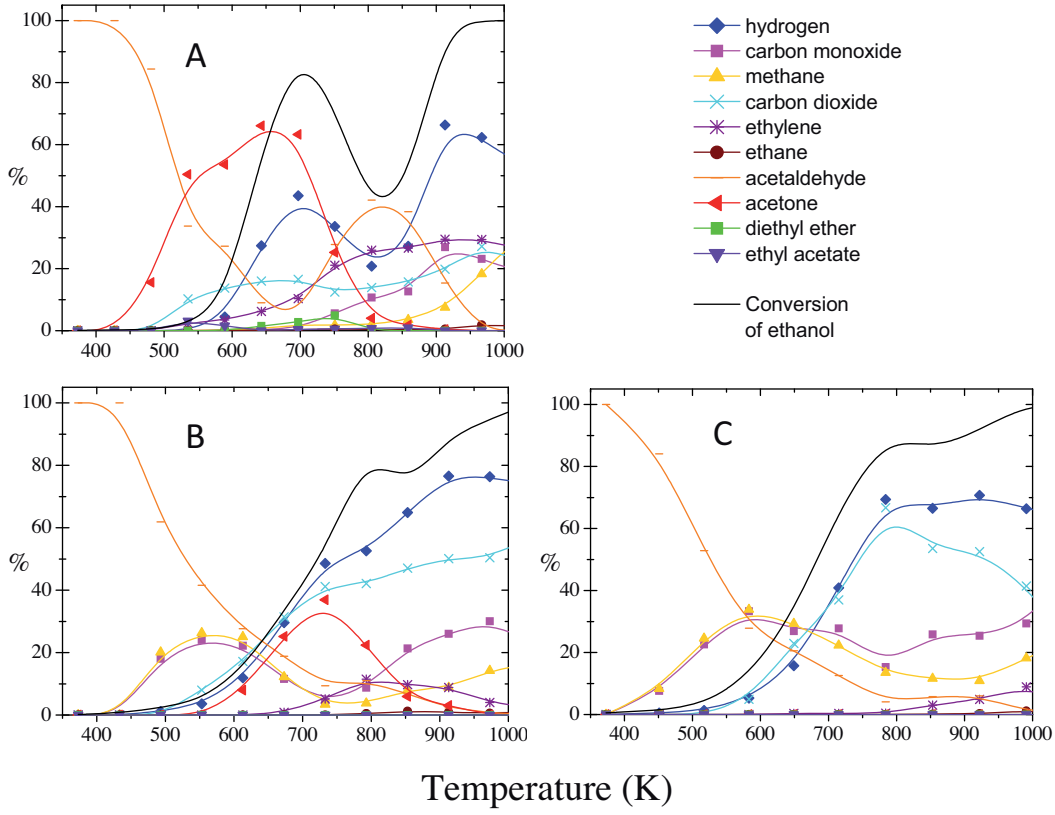

Fig. 2. Selectivities as a function of temperature in the ethanol–water steam reforming reaction (1:3 ratio) performed with linear heating (3 K/min) from 373 to 800 K. (A) 2% Co/ceria, (B) 0.1% Rh/ceria and (C) 0.1% Rh + 2% Co/ceria catalyst.

of cobalt was observed earlier on alumina supported Co catalyst [12,39,40]. It was assumed that hydrogen reduced the noble metal first, was activated on it, and spillover led to the increase of the reducibility of Co [39]. Another explanation can be that in the presence of noble metal changes of the crystal size resulted higher reducibility. Zhang et al. [41] found by means of XPS and XRD that a minor amount of Rh can preserve the dispersion of Co on alumina and this way also hinders the deactivation of the catalyst in methane dry reforming reaction.

The second important result of the electron spectroscopic measurements is that trace amounts of rhodium significantly altered the oxidation states of cobalt and ceria during the ethanol–water (SRE) reaction (Figs. 1B, 5A and 6B). Interestingly, after SRE reaction at 473–623 K, where acetaldehyde, methane and carbon monoxide were the dominant products, the cobalt was re-oxidized (Figs. 5A and 6B). The most intensive peak was detected for Co^{2+}, and the satellite strengthened at 786.2 eV. The existence of this satellite indicates that the cobalt oxidation state is mainly +2 at this temperature range and only a much smaller component could

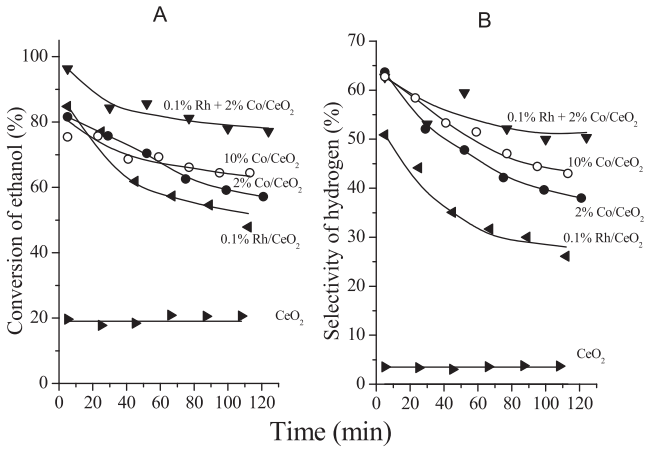

Fig. 3. Conversion of ethanol (A) and selectivity for hydrogen (B) as a function of reaction time at 723 K on 2% Co/CeO_2 (●), 10% Co/CeO_2 (○), 0.1% Rh + 2% Co/CeO_2 (▼), 0.1% Rh/CeO_2 (◄) and CeO_2 (►) catalysts.

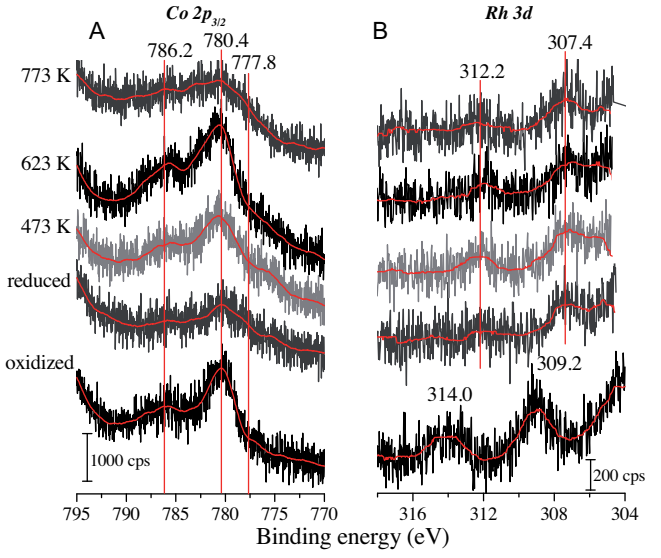

Fig. 4. Co 2p spectra after ethanol–water steam reforming reaction at different temperatures on 2% Co/ceria catalyst (A) and Rh 3d spectra on 0.1% Rh/ceria catalyst. The spectra after oxidation and reduction pretreatment are also shown.

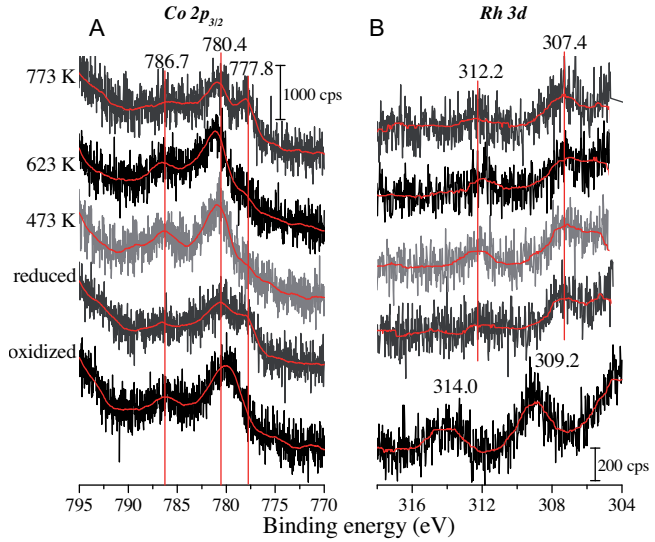

Fig. 5. Co 2p spectra after ethanol–water steam reforming reaction at different temperatures on 0.1% Rh + 2% Co/ceria catalyst (A) and Rh 3d spectra on 0.1% Rh + 2% Co/ceria catalyst. The spectra after oxidation and reduction pretreatment are also shown.

be detected for metallic cobalt (777.8 eV). The signature of Co^{3+} is a Co $2p_{3/2}$ peak at 780–781 eV with no satellite [29,31]. These observation evidenced that this re-oxidation occurs through is the formation of water-induced Co oxides under reaction condition. Very recently Lin and co-workers [42] found such kind of process on a very similar system (supported cobalt/ceria–zirconia catalysts) under ethanol steam reforming conditions. When the reaction temperature was increased to 773 K, where the hydrogen production is dominated, a significant fraction of metallic Co appeared again (Fig. 5A and Fig. 6B). Similar re-oxidation and reduction steps were detected by XRD on Co/ceria during ESR [9]. As it was expected Rh remained in reduced state on bimetallic catalyst at any reaction temperature (Fig. 5B). It is worth mentioning that the reduction degree of ceria is increased up slightly up to 773 K during reaction. The Ce^{3+} concentration after 773 K reaction was 17% (Fig. 1B).

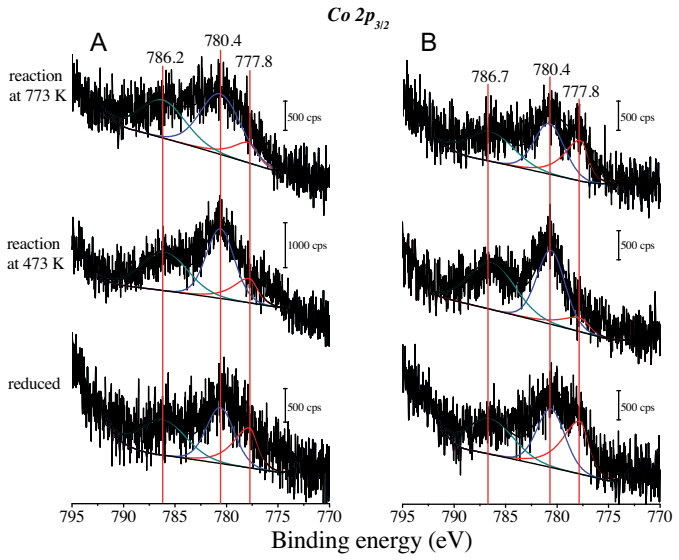

Fig. 6. Peak fitting for selected Co $2p_{3/2}$ of Figs. 4 and 5. Co $2p_{3/2}$ after reduction and after reaction at different temperatures; 2% Co/ceria (A) and 0.1% Rh + 2% Co/ceria (B).

From our observations we conclude that the promoter Rh has at least two different roles in this catalytic system. First, the reduction of Co (and CeO_2) in H_2 was much more efficient in the presence of Rh due to the hydrogen spillover phenomena [34]. Since H_2 is also present as a product, Rh may also help to keep the cobalt in the metallic state. On the other hand, Rh promotes the C—C bond scission reaction of ethanol, producing adsorbed CH_3 [3,43]. This is in agreement with the fact that on our Rh-containing samples the selectivity of methane is higher than on the CeO_2 and Co/CeO_2 systems. Taking into account these observations, we propose that Reactions (3) and (4) are the main reaction steps on 0.1% Rh + 2% Co/CeO_2 catalyst, followed by Reactions (5)–(7):

$$CH_{3(ads)} \rightarrow C_{(ads)} + H_{(ads)} + H_{2(g)} \quad (7)$$

$$CH_{3(ads)} + H_{(ads)} \rightarrow CH_{4(g)} \quad (8)$$

$$2H_{(ads)} \rightarrow H_{2(g)} \quad (9)$$

The fact that the bimetallic catalyst was the most active and selective in hydrogen production and at the same time it contained the largest fraction of Co in metallic state indicates that metallic cobalt sites are active in the SRE reaction. The bimetallic catalyst with ethanol–water mixture represents an interesting redox system. There are a Rh assisted cobalt reduction and a reoxidation step with water. Most likely, both Co^{2+} and metallic Co play roles in different steps of the SRE reaction. Supposedly, Co^{2+} is active in the dehydrogenation of ethanol at low temperatures (aldehyde formation), while metallic sites are particularly active above 700 K in C—C bond rupture and decarbonylation. The promoting effect of Rh was mainly rationalized by an increased efficiency in C—C bond scission and hydrogen formation on both Rh and metallic Co sites.

The amount and type of carbon formed in catalytic ethanol steam reforming is an important issue. Surface carbon is a know reaction product in the decomposition of ethanol [21]. In agreement with earlier findings [44], carbon deposits were formed covering both support and cobalt particles, regardless of the type of support used. The extent of coke formation and probably its surface structure depended on the support. In the case of pure ceria, in harmony with earlier findings [33,34] the formation of carbonaceous species is almost negligible. After 120 min of reaction at 823 K, the amount of deposited carbon on Co/CeO_2 was 344 μmol/g. Interestingly, although the Rh-promoted Co/CeO_2 showed the highest and most stable hydrogen selectivity, the amount of surface carbon, 1135 μmol/g, was higher than that on Co/CeO_2. Previous studies suggested that carbon build-up does not necessarily lead to deactivation [5,45,46]. In order to get more information about the type of carbonaceous species, we monitored the C 1s region before and after reaction at 473 and 773 K on Co/ceria and Rh promoted Co/ceria catalysts. On Co/ceria where the conversion was rather low, (473 K), the main C 1s component was detected at 284.5 eV (Fig. 7A). The intensity of this photoemission increased with increasing reaction temperature (773 K). Earlier electron microscopic results obtained on ceria-type supported Co catalyst revealed two types of carbon species: either carbonaceous layer on the surface of the grains, or filaments [46]. Presumably, these types of carbon can be detected at 284.5 eV binding energy. Very likely these types cannot be resolved in our XPS apparatus. A shoulder at the higher binding energy side at 286.3 eV can be attributed to chemisorbed ethanol/ethoxide. In harmony with the DRIFTS results these species are present up to 773 K [34]. The signals of the other carbon containing intermediates (aldehyde, acetate) overlap with the broad Ce 4s photoemission detected at 288.8 eV. Interestingly, at high reaction temperature, at which the conversion is high (~90–95%), a new C 1s peak developed at 282.3 eV (Fig. 7A). We attribute this photoemission to carbide-like species. Carbidic carbon at low binding energy was detected after potassium induced CO dissociation on Co foil [47], and carbidic carbon formation was

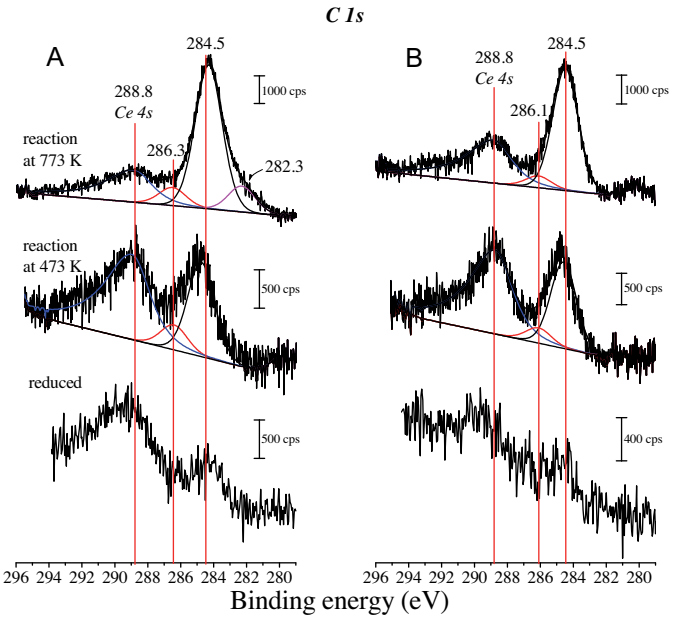

Fig. 7. C 1s spectra with Ce 4s contribution after ethanol–water steam reforming reaction at different temperatures on 2% Co/ceria (A) and on 0.1% Rh + 2% Co/ceria catalyst (B). C 1s region after hydrogen pretreatment is also shown in both cases.

observed with C 1s peak maximum at 282.3 eV on Si(1 0 0) during the decomposition of $Co_2(CO)_8$ [48].

A similar C 1s series is displayed in Fig. 7B for 0.1% Rh + 2% Co/CeO_2 catalyst. The carbonaceous layer and filaments structure appeared at 284.5 eV. The species due to C—O bond (286.3 eV) was detected with less intensity, indicating that ethoxide stability is limited on this surface [34]. It is very remarkable that carbide-like species does not form on this catalyst during ethanol steam reforming. It was pointed out earlier that the decreasing activity is related to the formation of carbon filaments [46]. In the light of our results we may conclude that the accumulation of strongly bonded carbide species in the case of Co/CeO_2 catalyst can contribute to the decreasing activity. This type of carbon is absent in the presence of trace amounts of Rh, therefore the catalyst was more stable.

4. Conclusions

Combined X-ray photoelectron spectroscopic and gas chromatographic experiments were carried out to find a relationship between the efficient H_2 production from EtOH + H_2O mixture (SRE) and the oxidation state of ceria supported Co–Rh catalysts. According to the results, CeO_2 alone also had a slight activity in the reaction, but on mono- and bimetallic Co–Rh samples the conversion and H_2 selectivity were much higher. Because of the re-oxidation of Ce^{3+} center by water, we could not follow the reaction mechanism by means of Ce 3d spectra on Co/ceria catalyst. Cobalt sintered during the pre-reaction, but under reaction it disrupted, and re-oxidized. In this stage acetone formation was dominant, so it can be concluded that oxidized centers are needed for aldol condensation. For 0.1% Rh + 2% Co/ceria rhodium remained in metallic state after reduction, and it enhanced the reduction of Co and slightly induced the reduction of ceria, too. On heating in EtOH + H_2O mixture, Co was being partially reduced and increasing H_2 production could be detected. At the same time, in the presence of rhodium in Co/ceria catalyst, the acetone formation was hindered. The promoting effect of Rh was mainly rationalized by an increased efficiency in C—C bond rupture on both Rh and metallic Co sites. Finally we can conclude that the Rh promoted Co/CeO_2 catalyst is the most appropriate for hydrogen production above 700 K in ethanol steam reforming due to its high metal Co content, but Co^{2+} is also necessary for the low temperature reaction, probably because of its dehydrogenation activity in which the aldehyde is the main reaction product. In the light of our results we may suggest that the accumulation of strongly bonded carbide species in the case of Co/CeO_2 catalyst can contribute to the decreasing activity. This type of carbon is absent in the presence of trace amounts of Rh, therefore the catalyst was more stable.

Acknowledgements

The financial support by the Alexander von Humboldt Foundation within the Research Group Linkage Program, by COST Action CM1301, by TÁMOP-4.2.2.A-11/1KONV-2012-0047 is acknowledged. The authors wish to thank Mrs. Kornélia Baán for the preparation and characterization of the catalysts.

References

[1] L.F. Brown, Int. J. Hydrogen Energy 26 (2001) 381–397.
[2] A. Haryanto, S. Fernando, N. Murali, S. Adhikari, Energy Fuels 19 (2001) 2098–2106.
[3] P.R. de la Piscina, N. Homs, Chem. Soc. Rev. 37 (2008) 2459–2467.
[4] A. Yee, S.J. Morrison, H. Idriss, Catal. Today 63 (2000) 327–335.
[5] L.V. Mattos, B.H. Jacobs, F.B. Noronha, Chem. Rev. 112 (2012) 4094–4123, and references therein.
[6] J. Llorca, N. Homs, P.R. de la Piscina, J. Catal. 227 (2004) 556–560.
[7] S.S.-Y. Lin, D.H. Kim, S.Y. Ha, Catal. Lett. 122 (2008) 295–301.
[8] H. Song, U.S. Ozkan, J. Mol. Catal. A 318 (2010) 21–29.
[9] B. Bayram, I.I. Soykal, D. Deak, J.T. Miller, U.S. Ozkan, J. Catal. 284 (2011) 77–89.
[10] I.I. Soykal, H. Sohn, U.S. Ozkan, ACS Catal. 2 (2012) 2335–2348.
[11] S.S. Itkulova, G.D. Zakumbaeva, A.A. Mukazhanova, Y.Y. Nurmakov, Cent. Eur. J. Chem. 12 (2014) 1255–1261.
[12] Zs. Ferencz, K. Baán, A. Oszkó, Z. Kónya, T. Kecskés, A. Erdőhelyi, Catal. Today 228 (2014) 123–130.
[13] M. Badlani, I.E. Wachs, Catal. Lett. 75 (2001) 137–149.
[14] A. Erdőhelyi, J. Raskó, T. Kecskés, M. Tóth, M. Dömök, Catal. Today 116 (2006) 367–376.
[15] M. Dömök, M. Tóth, J. Raskó, A. Erdőhelyi, Appl. Catal. B: Environ. 69 (2006) 262–272.
[16] A. Yee, S.J. Morrison, H. Idriss, J. Catal. 186 (1999) 279–295.
[17] J. Kaspar, P. Fornasiero, M. Graziani, Catal. Today 50 (1999) 285–298.
[18] A. Trovarelli, Catalysis by Ceria and Related Materials, Imperial College Press, London, 2002, pp. 1–528.
[19] A.M. da Silva, K.R. Souza, L.V. Mattos, G. Jacobs, B.H. Davis, F.B. Noronha, Catal. Today 164 (2011) 234–239.
[20] M. Happel, J. Myslivecek, V. Johánek, F. Dvorak, O. Stetsovych, Y. Lykhach, V. Matolín, J. Libuda, J. Catal. 289 (2012) 118–126.
[21] M. Mavrikakis, M. Barteau, J. Mol. Catal. 131 (1998) 135–147.
[22] C. Diagne, H. Idriss, A. Kiennemann, Catal. Commun. 3 (2002) 565–571.
[23] P.-Y. Sheng, A. Yee, G. Bowmaker, H. Idriss, J. Catal. 208 (2002) 393–403.
[24] M. Tóth, M. Dömök, J. Raskó, A. Hancz, A. Erdőhelyi, Chem. Eng. Trans. 4 (2004) 229–234.
[25] J. Raskó, M. Dömök, K. Baán, A. Erdőhelyi, Appl. Catal. A 299 (2006) 202–211.
[26] J. Raskó, J. Kiss, Appl. Catal. A 287 (2005) 252–260.
[27] C.J. Weststrate, H.J. Gericke, M.W.G.M. Verhoeven, I.M. Ciobica, A.M. Saib, J.W. Niemantsverdriet, J. Phys. Chem. Lett. 1 (2011) 1767–1770.
[28] D.R. Mullins, S.D. Senanayake, T.-L. Chen, J. Phys. Chem. C 114 (2010) 17112–17119.
[29] E. Martono, J.M. Vohs, J. Catal. 291 (2012) 79–86.
[30] E. Martono, M.P. Hyman, J.M. Vohs, Phys. Chem. Chem. Phys. 13 (2011) 9880–9886.
[31] M.-P. Hyman, J.M. Vohs, Surf. Sci. 605 (2011) 383–389.
[32] M.S. Batista, R.K.S. Santos, E.M. Assaf, J.M. Assaf, E.A. Ticinalli, J. Power Sources 124 (2003) 99–103.
[33] L. Óvári, S. Krick Calderon, Y. Lykhach, J. Libuda, A. Erdőhelyi, C. Papp, J. Kiss, H.-P. Steinrück, J. Catal. 307 (2013) 132–139.
[34] Zs. Ferencz, A. Erdőhelyi, K. Baán, A. Oszkó, L. Óvári, Z. Kónya, C. Papp, H.-P. Steinrück, J. Kiss, ACS Catal. 4 (2014) 1205–1218.
[35] A. Gazsi, A. Koós, T. Bánsági, F. Solymosi, Catal. Today 160 (2011) 70–80.
[36] P. Burroughs, A. Hamnett, A.F. Orchard, G. Thornton, Chem. Soc. Dalton Trans. 17 (1976) 1686–1698.
[37] D.R. Mullins, S.H. Overbury, D.R. Huntley, Surf. Sci. 409 (1998) 307–319.
[38] H. Idriss, C. Diagne, J.P. Hinderman, A. Kiennemann, M.A. Barteau, J. Catal. 155 (1995) 219–237.
[39] K.M. Cook, S. Poudyal, J.T. Miller, C.H. Bartholomew, Appl. Catal. A: Gen. 449 (2012) 69–80.
[40] G. Jacobs, T.K. Das, Y. Zhang, J. Li, G. Racoille, B.H. Davis, Appl. Catal. A: Gen. 233 (2002) 263–281.
[41] Y. Zhang, L. Chen, G. Bai, Y. Li, X. Yan, J. Catal. 236 (2005) 176–180.

[42] S.S.-Y. Lin, D.H. Kim, M.H. Engelhard, S.-Y. Ha, J. Catal. 273 (2010) 229–235.
[43] J. Zhang, Z. Zhong, X.-M. Cao, P. Hu, M.B. Sullivan, L. Chen, ACS Catal. 4 (2014) 448–456.
[44] B.G. Johnson, C.H. Bartholomew, D.W. Goodman, J. Catal. 128 (1991) 231–247.
[45] J.M. Guil, N. Homs, J. Llorca, P.R. de la Piscina, J. Phys. Chem. B 109 (2005) 10813–10819.
[46] J.C. Vargas, S. Libs, A.C. Roger, A. Kiennemann, Catal. Today 107 (2005) 417–425.
[47] D.A. Wesner, G. Linden, H.P. Bonzel, Appl. Surf. Sci. 26 (1986) 335–356.
[48] D.-X. Ye, S. Pimanpang, C. Jezewski, F. Tang, J.J. Senkevich, G.-C. Wang, T.-M. Lu, Thin Solid Films 485 (2005) 95–100.